



Low-field cross spin relaxation of ^8Li in superconducting NbSe_2

M. D. Hossain,¹ Z. Salman,² D. Wang,¹ K. H. Chow,³ S. Kreitzman,² T. A. Keeler,¹ C. D. P. Levy,² W. A. MacFarlane,⁴ R. I. Miller,² G. D. Morris,² T. J. Parolin,⁴ M. Pearson,² H. Saadaoui,¹ and R. F. Kiefl^{1,2,5}

¹*Department of Physics and Astronomy, University of British Columbia, Vancouver, British Columbia, Canada V6T 1Z1*

²*TRIUMF, 4004 Wesbrook Mall, Vancouver, British Columbia, Canada V6T 2A3*

³*Department of Physics, University of Alberta, Edmonton, Alberta, Canada T6G 2G7*

⁴*Department of Chemistry, University of British Columbia, Vancouver, British Columbia, Canada V6T 1Z1*

⁵*Canadian Institute for Advanced Research, Toronto, Ontario, Canada M5G 1Z8*

(Received 18 November 2008; revised manuscript received 27 February 2009; published 22 April 2009)

A low energy beam of spin polarized ^8Li has been used to investigate nuclear spin relaxation in the multiband superconductor NbSe_2 . In low magnetic fields there is significant cross relaxation between the ^8Li and the host ^{93}Nb spins, which is driven by low frequency fluctuations in the nuclear magnetic dipolar interaction. The rate of cross relaxation is strongly field dependent and thus the $1/T_1$ spin relaxation rate of the ^8Li is a sensitive monitor of the static local magnetic field B just below the surface. This in turn is used to determine the absolute value of the magnetic penetration depth λ in the Meissner state. The temperature variations in $1/T_1$ and λ are consistent with a wide distribution of superconducting gaps expected for a multiband superconductor.

DOI: [10.1103/PhysRevB.79.144518](https://doi.org/10.1103/PhysRevB.79.144518)

PACS number(s): 74.25.Qt, 74.25.Ha, 76.75.+i, 76.60.-k

I. INTRODUCTION

NbSe_2 belongs to a family of transition metal dichalcogenides and exhibits interesting physical properties such as superconductivity ($T_c=7.0$ K) and a charge density wave ($T_{\text{CDW}}=30$ K). Its layered crystal structure gives rise to a strong anisotropy in both its electronic and mechanical properties.¹ There is also recent evidence^{2,3} that the superconductivity is multiband, whereby different parts of the Fermi surface have different superconducting gaps.⁴ This may lead to unusual properties in the vortex state. For example, delocalized quasiparticles associated with the vortices are believed to be responsible for the anomalous thermal conductivity in a magnetic field⁵ and also for the enlarged vortex cores.⁶ Vortex structure and vortex interactions are interesting but complicate the theory for the magnetic field distribution in the vortex state. This can lead to uncertainty in the absolute value of the London penetration depth derived from muon spin rotation/relaxation μSR (Refs. 7–9) and $\beta\text{-NMR}$ (Ref. 10) in the vortex state. The magnetic field distribution in the Meissner state is less complicated and thus a measurement of λ is more direct. So far this has only been possible with low energy muons on large area thin films.^{11,12}

In this paper we investigate the longitudinal relaxation rate $1/T_1$ of ^8Li nuclear spins in the Meissner state of a single crystal of NbSe_2 . We show that in low magnetic fields $1/T_1$ is driven by low frequency host nuclear spin dynamics, principally ^{93}Nb . A characteristic Lorentzian field dependence in $1/T_1$ is observed and attributed to fluctuations in the magnetic dipolar interaction between the ^8Li and neighboring ^{93}Nb nuclear spins. The observed $1/T_1$ spin relaxation rate of ^8Li is sensitive to the static local magnetic field and the host ^{93}Nb $1/T_1$ spin relaxation rate at a well-defined mean depth below the surface. Below T_c a sharp increase in $1/T_1$ is observed which is used to measure the absolute value of the London penetration depth in the a - b plane λ_{ab} . The temperature dependence of λ_{ab} is considerably different from

the empirical two fluid model which characterizes many single gap superconductors. Furthermore, the Hebel-Slichter peak¹³ in $1/T_1$ just below T_c is small and broad. Both of these effects are consistent with a distribution of superconducting gaps.

II. EXPERIMENTAL

The 28 keV beam of ^8Li is produced at the isotope separator and accelerator (ISAC) at TRIUMF. A large nuclear polarization (70%) is generated in flight using a collinear optical pumping method.¹⁴ The polarized beam is bent 90° and directed into a recently commissioned low field $\beta\text{-NMR}$ spectrometer. The mean depth of the implanted ^8Li in this experiment was fixed at 120 nm, although in future studies it will be possible to vary the implantation depth over a wide range of 2–200 nm.

A schematic of the apparatus is shown in Fig. 1. Helmholtz coils are used to apply a small uniform magnetic field from 0 to 15 mT in the \hat{y} direction, which is parallel to both the sample surface and initial ^8Li polarization. In $\beta\text{-NMR}$ the nuclear polarization is monitored through the anisotropic β decay of a radioactive nucleus. In this case the probe is ^8Li , which has nuclear spin ($I=2$) and a mean lifetime $\tau=1.2$ s. The emitted beta has an average energy of about 6 MeV so it can easily pass through thin stainless steel windows in the ultrahigh vacuum (UHV) chamber and reach the surrounding plastic scintillation detectors.¹⁵

The single crystal of $2H\text{-NbSe}_2$ measured about 4 mm in width and length in the ab plane and 0.1 mm along the hexagonal c axis. Magnetization measurements showed a superconducting transition at $T_c=7.0$ K with a 10%–90% transition width in 0.1 K. Immediately prior to introducing it into the UHV chamber (10^{-9} torr) the sample was attached to a sapphire plate and cleaved. It was then mounted on a cold finger cryostat with the c axis along the beam direction. The

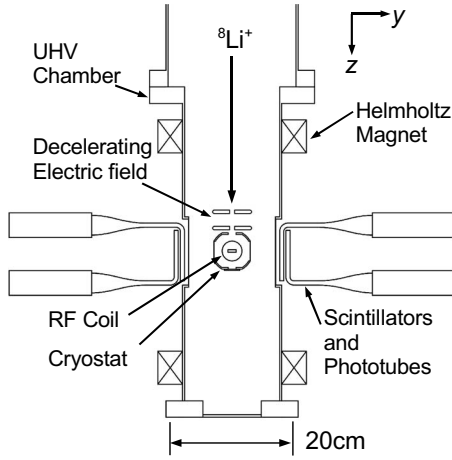


FIG. 1. Experimental setup used to measure the spin relaxation rate of ^8Li in low magnetic fields. The initial polarization and small external magnetic field are in the \hat{y} direction. The cryostat is held from above on a high voltage platform which will be used in the future to control the mean depth of implantation.

beam was focused such that there was no detectable background signal.¹⁰

A long pulse method^{16–18} was used to measure $1/T_1$ of the ^8Li , in which a period of 4 s of beam on is followed by 12 s of beam off. Figure 3 shows the typical time dependence of the beta-decay asymmetry $A\mathcal{P}(t)$ over the full time interval, where A is an experimental constant determined by the properties of the beta decay, geometry, and degree of polarization and $\mathcal{P}(t)$ is the nuclear polarization averaged over all ^8Li in the sample and normalized such that $\mathcal{P}(0)=1$. The form of the relaxation function is explained below.

III. RESULTS

In a previous study of the normal state we have shown that there is no resolved quadrupolar splitting of the β -NMR resonance of ^8Li in NbSe_2 .¹⁹ A typical resonance is shown in Fig. 2. Both the Knight shift and Korringa relaxation rate

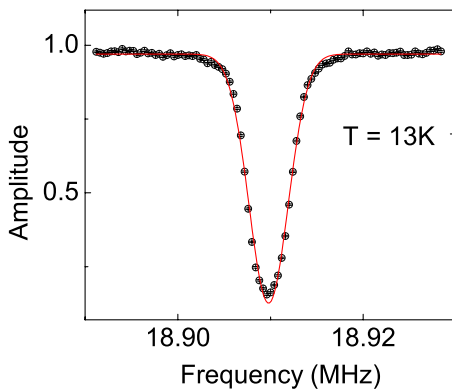


FIG. 2. (Color online) The nuclear resonance spectrum of ^8Li in the normal state of NbSe_2 in a high magnetic field of 30 kG. The linewidth is attributed to magnetic dipolar broadening from host ^{93}Nb nuclear moments. Note that there is no evidence for any quadrupolar splitting (see Ref. 19 for more details).

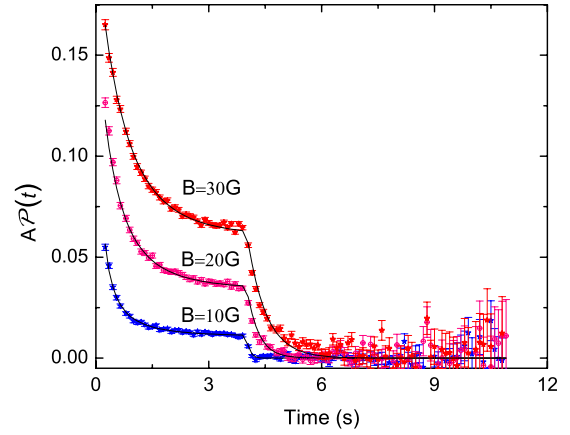


FIG. 3. (Color online) The time dependence of the nuclear polarization of ^8Li in the normal state of NbSe_2 at 8K at various magnetic fields. The fitted curves are generated by assuming a single exponential spin relaxation rate as explained in the text.

measured in a high magnetic field of 30 kG are very small indicating that there is little direct contact with the conduction electrons. This is evidence that the ^8Li occupies an interstitial position between the NbSe_2 layers. The observed Gaussian linewidth of 2.1 kHz is attributed to the magnetic dipolar broadening from the host ^{93}Nb nuclear spins.

In the current experiment the spin relaxation rate of ^8Li was investigated in weak magnetic fields, where the spin relaxation rate is much larger and strongly field dependent. Typical spin relaxation data in the normal state at 8 K are shown in Fig. 3. The measured asymmetry is maximum when the beam is first turned on and then approaches an equilibrium value $A/[1 + \tau/T_1]$, where τ is the mean lifetime of ^8Li and T_1 is its nuclear spin relaxation time. At $t=4$ s the beam goes off and the polarization decays exponentially to zero with the relaxation time T_1 . Excellent fits to the normal state data were obtained assuming single exponential relaxation for a ^8Li spin arriving at time t' , and detected later at time t , i.e., $p(t-t') = \exp[-(t-t')/T_1]$. The fitted curves are obtained by weighting $p(t-t')$ according to the radioactive decay of the ^8Li and integrating over arrival times $t' < t$.^{17,18} One then obtains an average polarization for all the ^8Li in the sample at time t ,

$$\mathcal{P}(t) = \frac{\tau'}{\tau} \times \frac{1 - \exp[-t/\tau']}{1 - \exp[-t/\tau]},$$

$$\mathcal{P}(t) = \frac{\tau'}{\tau} \times \frac{1 - \exp[-t_p/\tau']}{1 - \exp[-t_p/\tau]} \exp[-(t-t_p)/T_1] \quad (1)$$

depending on whether $t < t_p$ or $t > t_p$, respectively, where t_p is the pulse length, τ is the mean ^8Li lifetime, T_1 is the spin relaxation time, and $1/\tau' = 1/\tau + 1/T_1$.

Figure 4 shows the magnetic field dependence of the fitted $1/T_1$. This is very different than the behavior in high magnetic fields (e.g., 30 kG) where the ^8Li $1/T_1$ is 1 order of magnitude smaller and independent of the applied magnetic field. The enhanced relaxation and its strong dependence on magnetic field are attributed to cross relaxation with the host

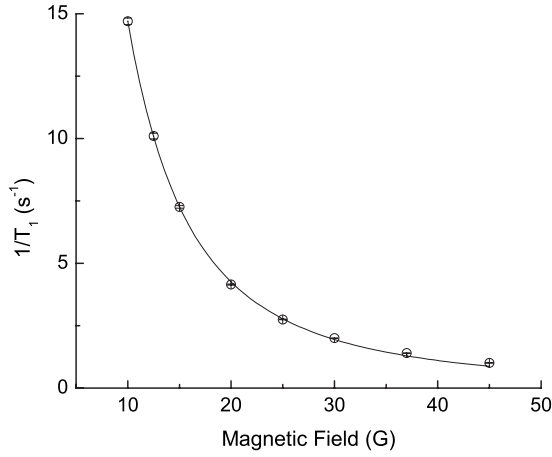


FIG. 4. The $1/T_1$ spin relaxation rate of ^8Li as a function of magnetic field at 8 K. The curve is a fit to a simple Lorentzian corresponding to an exponential time correlation function for the nuclear dipolar fields from the host Nb nuclear spins.

^{93}Nb spins which is driven by low frequency fluctuations in the magnetic dipolar interaction. Essentially the ^8Li nuclear polarization is being transferred to the host ^{93}Nb nuclear spins at a rate equal to $1/T_1$. In high magnetic fields this contribution to the ^8Li spin relaxation is completely quenched, except near level crossing resonances,²⁰ whereas in low fields it is dominant. The behavior in low field may also be considered a level crossing resonance except when the resonance in this case occurs it occurs at zero magnetic field. The origin of the cross relaxation is the same in zero field as it is for a level crossing resonance at a finite field. The curve is a fit to a simple Lorentzian form, corresponding to an exponential autocorrelation function of the fluctuating local magnetic dipolar field,

$$\frac{1}{T_1} = \frac{(\gamma B_d)^2 \tau_c}{1 + (\gamma B \tau_c)^2}, \quad (2)$$

where $\gamma = 2\pi \times 630$ Hz/G is the gyromagnetic ratio of ^8Li , B_d is the magnitude of the fluctuating dipolar field, B is the applied field, and τ_c is the correlation time for fluctuations in B_d from ^{93}Nb spins.²¹ In the slow fluctuation limit $1/T_1$ [$\approx B_d^2 / (B^2 \tau_c)$] varies inversely with B^2 and is proportional to $1/\tau_c$. The fit to Eq. (2) yields a value for $B_d^2 / \tau_c = 1800(30)$ $\text{G}^2 \text{s}^{-1}$. From the β -NMR resonance linewidth in the normal state¹⁹ (see Fig. 2) we can make an estimate of $B_d \approx 2.0(5)$ G, yielding $1/\tau_c = 450(200)$ s^{-1} at 10 K. As explained below this is in reasonable agreement with what is expected from conventional measurements of the host ^{93}Nb spin relaxation times T_1 and T_2 .

The low field cross spin relaxation rate of ^8Li is also a strong function of temperature. Figure 5 shows how the time evolution of the nuclear polarization $AP(t)$ changes above and below the superconducting transition temperature with a small magnetic field of 30 G applied parallel to the surface, which is much smaller than the lower critical field of 600 G.²² Note the increased relaxation below $T_c = 7.0$ K, which is attributed to screening of the applied field by induced supercurrents. All the measurements are performed under zero-

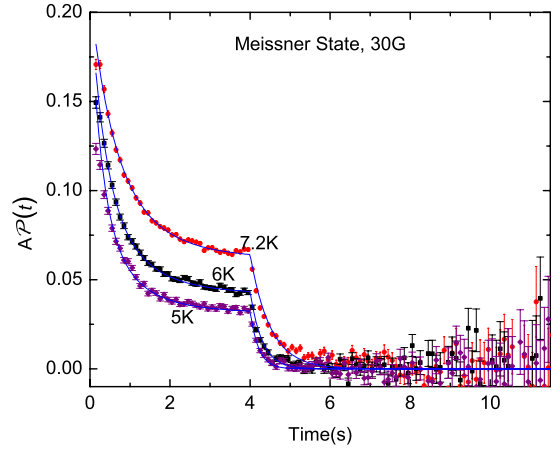


FIG. 5. (Color online) Low-field nuclear spin relaxation of ^8Li in NbSe_2 above and below $T_c = 7.0$ K. A magnetic field of 30 G, which is much less than H_{c1} (Ref. 22), is applied parallel to the surface after zero-field cooling. Note the sharp increase in the relaxation rate below the transition temperature. This is attributed to the Meissner screening of the external field. The size of the increase is a direct measure of the London penetration depth near the surface.

field-cooled conditions with the external field aligned to within about 0.2° parallel to the surface, ensuring that the entire sample is in the Meissner state.

The open circles in Fig. 6 show a sharp rise in the average spin relaxation rate below T_c which is attributed shielding of the applied field in the Meissner state. Together with the calculated stopping distribution [see $\rho(x)$ in Fig. 7] and measured field dependence of $1/T_1$ (Fig. 4), this increase provides a direct measure of the London penetration depth. One

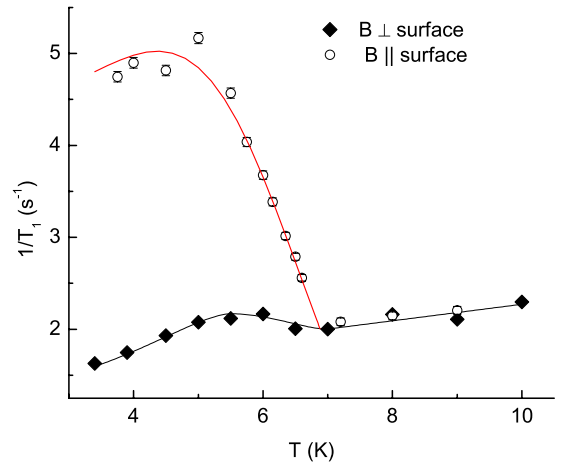


FIG. 6. (Color online) The temperature dependence of the $1/T_1$ of ^8Li in NbSe_2 with a small external magnetic field of 30 G applied parallel to the surface (open circles) and with a 100 G applied perpendicular to the surface (filled diamonds). The fitted curve through the vortex state data (filled diamonds) is based on the Hebel-Slichter theory assuming a multigap model as described in the text. The curve through the Meissner state data (open circles) is also derived from this model, taking into account the reduction in magnetic field from Meissner screening, using the temperature dependent London penetration depth given in Fig. 8.

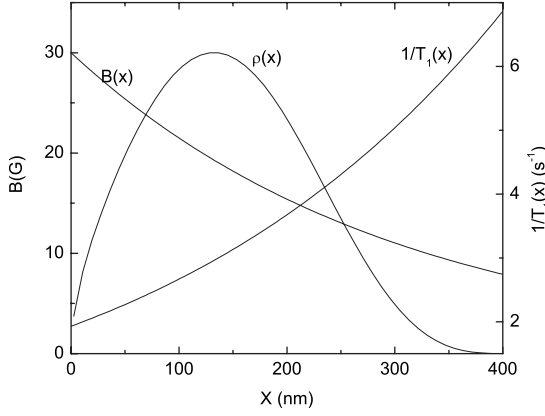


FIG. 7. The depth dependence of the magnetic field $B(x)$, the stopping density $\rho(x)$, and the spin relaxation rate $1/T_1(x)$.

can make a simple estimate of λ_{ab} as follows: extrapolate the linear variation $1/T_1$ in the normal state (shown in Fig. 6) to a temperature below T_c to obtain an estimate for the shift in τ_c from just above T_c to below T_c . (Note that the temperature variation in τ_c is small and thus has only a minor effect on resulting value of λ_{ab} .) Using the measured value of $1/T_1$ below T_c one can solve Eq. (2) to estimate the average local field $\langle B(x) \rangle$. One can then solve the London equation $\langle B(x) \rangle = B(0) \exp[-x/\lambda_{ab}]$ for λ_{ab} using the average stopping depth $\langle x \rangle$ from Fig. 7. For example at 4 K this procedure gives an average magnetic field of $\langle B(x) \rangle = 16.4(1)$ G, which is substantially less than the applied field of $B_0 = 30$ G. The reduction corresponds to a London penetration depth of $243(3)$ nm at 4 K, which is close to the value obtained using the more sophisticated analysis described below.

IV. ANALYSIS AND DISCUSSION

More accurate values of λ_{ab} and its variation with temperature can be obtained by fitting the time dependence of the polarization at each temperature (see Fig. 5) taking into account the stopping distribution and resulting spread of relaxation rates. The stopping distribution $[\rho(x)]$ calculated using TRIM-SP,²³ the expected exponential decay of the magnetic field $B(x) = B_0 \exp[-x/\lambda_{ab}]$ in the Meissner state, and a resulting depth dependent relaxation rate $1/T_1(x)$ are all shown in Fig. 7. Each of the time spectra below T_c (e.g., Fig. 5) was fit to a depth averaged polarization function,

$$\langle \mathcal{P}(t) \rangle = \int \rho(x) \mathcal{P}(x, t) dz, \quad (3)$$

where $\mathcal{P}(x, t)$ is given by Eq. (1) using a depth dependent $1/T_1$ given by Eq. (2) and the London model for $B(x) = B_0 \exp[-x/\lambda_{ab}]$. In addition, a small correction to τ_c at each temperature was made using data taken in the vortex state (filled diamonds in Fig. 6). In this geometry the temperature dependence of $1/T_1$ is governed solely by that of τ_c as described below. As one can see from Fig. 5, the theoretical expression for the relaxation function in the Meissner state gives an excellent fit to the data below T_c . The only free parameters are λ_{ab} and the initial polarization. The fitted

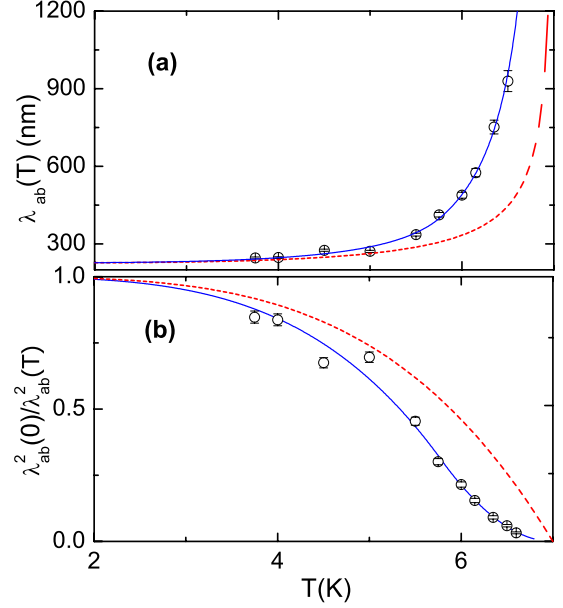


FIG. 8. (Color online) (a) The magnetic penetration depth λ_{ab} in the Meissner state of NbSe₂ as a function of temperature. The solid lines are a fit to the multigap model, whereas the dashed line is a fit to the single gap model given by Eq. (4). (b) The inverse square of the penetration depth versus temperature normalized the value at $T=0$.

temperature dependence of λ_{ab} is shown in Fig. 8(a). Using the fact that $1/\lambda_{ab}^2(T) = 4\pi n_s/mc^2$, where n_s is the superfluid density, one can also plot the temperature dependence of the normalized superfluid density $n_s(T)/n_s(0) = \lambda_{ab}^2(0)/\lambda_{ab}^2(T)$ [see Fig. 8(b)]. In both plots the dashed curves show the phenomenological power-law form that is observed in many single gap BCS superconductors,¹

$$\lambda_{ab}(T) = \lambda_{ab}(0) \left[1 - \left(\frac{T}{T_c} \right)^4 \right]^{-1/2}. \quad (4)$$

The solid curves are a fit to a simple model for a minimally coupled multiband superconductor assuming a square distribution of gaps. In the limit of zero coupling there is a corresponding square distribution of T_c 's all with the same value of $2\Delta/k_B T_c$.⁴ In reality there is always some coupling so there is single transition temperature. However when the coupling is small the density of states approaches our simple model with a distribution of T_c 's. In the fit the range of T_c is from T_c^{\min} to $T_c = 7.0$ K. In the multigap model the penetration depth $\lambda_{ab}(T) = 1/\sqrt{\langle 1/\lambda_{ab}^2(T, \Delta) \rangle}$ where the angled brackets indicate an average over the gap distribution. Thus at any given temperature only gapped parts of the Fermi surface contribute to the superfluid density. The best fit gives $T_c^{\min} = 5.78(4)$ K and $\lambda_{ab}(0) = 226(3)$ nm. Note that in the multigap model, the superfluid density in Fig. 8(b) evolves more slowly than the single gap model. It is likely that there are other contributions to the unusual temperature dependence in λ such as gap anisotropy. However these alone would not be consistent with scanning tunneling microscopy (STM) (Ref. 2) and angle-resolved photoemission spectroscopy (ARPES) data,³ both of which show that a significant fraction of the

Fermi surface appears gapless above 5 K. Also the multigap model is a natural explanation for the small Hebel-Slichter peak shown by the filled diamonds in Fig. 6. It should be noted that STM and ARPES are very surface sensitive where the present result characterizes the subsurface region. The unusual temperature dependence of the normalized superfluid density in Fig. 8(b) is similar to rf resonant circuit precision measurements of the temperature dependence of λ which find evidence for two gaps.²⁴ However, in that case the temperature dependence of the superfluid density relies on other measurements of the absolute value of $\lambda_{ab}(0)$. Our measured value of $\lambda_{ab}(0)$ is close to what has been observed in the vortex state¹⁰ but in the present experiment there are no complications due to vortex structure or dynamics. There may be other systematic effects related to the surface properties. For example, low energy muon experiments on thin films typically find evidence for a thin dead layer of thickness $\delta \approx 2-20$, in which there is no shielding.^{11,12} In previous work on the vortex state we found no evidence for a superconducting dead layer in freshly cleaved NbSe_2 .¹⁰ Nevertheless we reanalyzed the data assuming a small nonzero δ . The temperature dependence of λ_{ab} is unaffected whereas the value of λ_{ab} at $T=0$ is reduced by an amount approximately equal to δ . In the future it will be possible to vary the energy of implantation and thereby measure the entire field profile and any possible dead layer. There are also plans to install a low temperature cryostat. These capabilities will allow more precise measurements of the absolute value of the penetration depth and its temperature dependence in many superconductors.

As mentioned above there is a slight temperature dependence in τ_c . This can be measured independently using a different geometry where the magnetic field is applied perpendicular to the surface. In this case the large demagnetization factor ensures that the sample enters the vortex state so that the average internal magnetic field is very close to the applied field.¹⁰ The resulting values of $(1/T_1)_\perp$ are the filled diamonds in Fig. 6 and have been scaled upward by a factor of 1.56 to overlap in the normal state with the $(1/T_1)_\parallel$ data. The scaling factor is attributed to the difference in the magnetic field and anisotropy in B_d and τ_c . In this geometry the average magnetic field is almost temperature independent and the same above and below T_c . There is broadening of the field distribution in the vortex state but this has little effect on the observed average relaxation rate at this magnetic field. The temperature dependence of $(1/T_1)_\perp$ is then attributed solely to changes in $1/\tau_c$. Above T_c $(1/T_1)_\perp$ is found to follow a simple linear form $a+bT$. The temperature independent term $a=1.37(17) \text{ s}^{-1}$ is attributed to fluctuations in B_d arising from the Nb-Nb spin-spin relaxation (^{93}Nb $1/T_2$), whereas the T -dependent term $b=8.9(2) \times 10^{-2} \text{ s}^{-1}/\text{K}$ is attributed to Korringa spin-lattice relaxation (^{93}Nb $1/T_1$). The contribution to $1/\tau_c$ from ^{93}Nb $1/T_1$ is approximately $bTB^2/B_d^2=200(100) \text{ s}^{-1}$ at 10 K. The form of the relaxation function for $S=9/2$ ^{93}Nb in NbSe_2 from nuclear quadrupole resonance (NQR) is multiexponential.²⁵ Nevertheless one can estimate an effective τ_c from ^{93}Nb $1/T_1$ as the time which the polarization drops to $1/e$ of its initial value. This gives $1/\tau_c \approx 130 \text{ s}^{-1}$ at 10 K. The agreement with the present experiment is reasonable considering the uncertain-

ties. Note that below T_c there is a broad feature which we attribute to a Hebel-Slichter coherence peak¹³ in the ^{93}Nb $1/T_1$. The peak is smaller and broader than an ideal BCS superconductor with a single superconducting gap and is consistent with NQR measurements of ^{93}Nb $1/T_1$ on a powdered sample.²⁵ There are many potential sources of broadening in the density of states which can lead to a reduced coherence peak.²⁶ The fitted curve below T_c is obtained from the multigap model assuming a square distribution of T_c 's from 5.9 to 7.0 K and a small quasiparticle damping rate of $\Gamma/k_B=0.36 \text{ K}$.^{26,27} It is interesting to note the ^8Li $1/T_1$ does not drop off exponentially at low temperatures, as in the case of conventional NQR measurements of the host ^{93}Nb $1/T_1$, but instead approaches a constant value determined by the ^{93}Nb $1/T_2$. This may be traced to the fact that in low magnetic fields the observed ^8Li $1/T_1$ is the rate at which polarization is being transferred to the host nuclear ^{93}Nb spin system rather than to the electronic spin system. Consequently the cross relaxation rate remains finite even at very low temperatures because the host nuclear spins continue to fluctuate via their spin-spin interaction.

An important aspect of the present paper is that it demonstrates a way to monitor host nuclear spin dynamics with an implanted spin probe. For example, most conventional NMR in superconductors is done on crushed powders in order to obtain a reasonable signal to noise ratio. Furthermore, in conventional NMR and NQR the signal comes from the entire rf penetration depth, which cannot be controlled easily. The current method offers a way to monitor host nuclear spin relaxation in single crystals and heterostructures as a function of depth. In particular we have shown that in low magnetic fields $1/T_1$ of the ^8Li is dominated by dynamics of the neighboring host nuclear spins which are coupled to the ^8Li through a magnetic dipolar interaction. The T -dependent part is from the host nuclear $1/T_1$, whereas the T -independent part is from the host $1/T_2$. The present experiment was performed at a fixed mean energy, but it is a straight forward extension to vary the depth of implantation. Thus it will be possible to monitor host nuclear spin dynamics as a function of depth on a nanometer length scale. A similar, but more subtle, effect also occurs at level crossing resonances, where it has been shown that the host nuclear spin dynamics can affect the level crossing resonance linewidths.²⁰ Finally, we expect that low energy β -NMR measurements of $1/T_1$ will be useful in measuring the depth and temperature dependence of the host $1/T_1$ in heterostructures and single crystals where conventional NMR and NQR are problematic at best and often impossible.

V. SUMMARY

In summary, low field cross relaxation between implanted ^8Li spins and host ^{93}Nb nuclear spins has been investigated in the Meissner state of a single crystal of NbSe_2 . The cross relaxation is driven by low frequency dynamics of the host ^{93}Nb nuclear spins and is a sensitive monitor of the local

magnetic field and the host nuclear spin relaxation rate at a well-defined mean depth beneath the surface. This is used to measure the absolute value of the London penetration depth λ_{ab} in NbSe₂. The temperature dependence of λ_{ab} differs substantially from the common two fluid model observed in many single gap superconductors. Also, there is evidence for a broad coherence peak in the host ⁹³Nb spin relaxation rate. Both effects are attributed to the multiband nature of the superconductivity in NbSe₂. We expect that this method can be applied more generally to monitor the host nuclear spin dynamics in single crystals and heterostructures as a function of depth and temperature.

ACKNOWLEDGMENTS

We would like to thank Doug MacLaughlin for a critical reading of the paper and Joe Brill at the University of Kentucky for providing the sample. This research was supported by the Center for Molecular and Materials Science at TRIUMF, the Natural Sciences and Engineering Research Council of Canada, and the Canadian Institute for Advanced Research. We would especially like to acknowledge Rahim Abasalti, Bassam Hitti, Donald Arseneau, and Suzannah Daviel for expert technical support.

-
- ¹C. P. Poole, H. A. Farach, and R. J. Creswick, *Superconductivity*, 2nd ed. (Academic, New York, 1995).
- ²J. G. Rodrigo and S. Vieira, *Physica C* **404**, 306 (2004).
- ³T. Yokoya, T. Kiss, A. Chainani, S. Shin, M. Nohara, and H. Takagi, *Science* **294**, 2518 (2001).
- ⁴H. Suhl, B. T. Matthias, and L. R. Walker, *Phys. Rev. Lett.* **3**, 552 (1959).
- ⁵E. Boaknin, M. A. Tanatar, J. Paglione, D. Hawthorn, F. Ronning, R. W. Hill, M. Sutherland, L. Taillefer, J. Sonier, S. M. Hayden, and J. W. Brill, *Phys. Rev. Lett.* **90**, 117003 (2003).
- ⁶F. D. Callaghan, M. Laulajainen, C. V. Kaiser, and J. E. Sonier, *Phys. Rev. Lett.* **95**, 197001 (2005).
- ⁷J. E. Sonier, M. F. Hundley, J. D. Thompson, and J. W. Brill, *Phys. Rev. Lett.* **82**, 4914 (1999).
- ⁸R. I. Miller, R. F. Kiefl, J. H. Brewer, J. Chakhalian, S. R. Dunsiger, G. D. Morris, J. E. Sonier, and W. A. MacFarlane, *Phys. Rev. Lett.* **85**, 1540 (2000).
- ⁹J. E. Sonier, J. H. Brewer, and R. F. Kiefl, *Rev. Mod. Phys.* **72**, 769 (2000).
- ¹⁰Z. Salman, D. Wang, K. H. Chow, M. D. Hossain, S. R. Kreitzman, T. A. Keeler, C. D. P. Levy, W. A. MacFarlane, R. I. Miller, G. D. Morris, T. J. Parolin, H. Saadaoui, M. Smadella, and R. F. Kiefl, *Phys. Rev. Lett.* **98**, 167001 (2007).
- ¹¹T. J. Jackson, T. M. Riseman, E. M. Forgan, H. Gluckler, T. Prokscha, E. Morenzoni, M. Pleines, Ch. Niedermayer, G. Schatz, H. Luetkens, and J. Litterst, *Phys. Rev. Lett.* **84**, 4958 (2000).
- ¹²A. Suter, E. Morenzoni, N. Garifanov, R. Khasanov, E. Kirk, H. Luetkens, T. Prokscha, and M. Horisberger, *Phys. Rev. B* **72**, 024506 (2005).
- ¹³L. C. Hebel and C. P. Slichter, *Phys. Rev.* **113**, 1504 (1959).
- ¹⁴C. D. P. Levy, R. Baartman, K. Jayamanna, R. Kiefl, T. Kuo, M. Olivo, G. W. Wight, D. Yuan, and A. N. Zelenski, *Nucl. Phys. A* **701**, 253 (2002).
- ¹⁵G. D. Morris, W. A. MacFarlane, K. H. Chow, Z. Salman, D. J. Arseneau, S. Daviel, A. Hatakeyama, S. R. Kreitzman, C. D. P. Levy, R. Poutissou, R. H. Heffner, J. E. Elenewski, L. H. Greene, and R. H. Kiefl, *Phys. Rev. Lett.* **93**, 157601 (2004).
- ¹⁶Yu. G. Abov, A. D. Gulko, and F. S. Dzherparov, *Phys. At. Nucl.* **69**, 1701 (2006).
- ¹⁷R. I. Miller, D. Arseneau, K. H. Chow, S. Daviel, A. Engelbertz, M. D. Hossain, T. Keeler, R. F. Kiefl, S. Kreitzman, C. D. P. Levy, P. Morales, G. D. Morris, W. A. MacFarlane, T. J. Parolin, R. Poutissou, H. Saadaoui, Z. Salman, D. Wang, and J. Y. T. Wei, *Physica B* **374-375**, 30 (2006).
- ¹⁸Z. Salman, R. F. Kiefl, K. H. Chow, M. D. Hossain, T. A. Keeler, S. R. Kreitzman, C. D. P. Levy, R. I. Miller, T. J. Parolin, M. R. Pearson, H. Saadaoui, J. D. Schultz, M. Smadella, D. Wang, and W. A. MacFarlane, *Phys. Rev. Lett.* **96**, 147601 (2006).
- ¹⁹D. Wang, M. D. Hossain, Z. Salman, D. Arseneau, K. H. Chow, S. Daviel, T. A. Keeler, R. F. Kiefl, S. R. Kreitzman, C. D. P. Levy, G. D. Morris, R. I. Miller, W. A. MacFarlane, T. J. Parolin, and H. Saadaoui, *Physica B* **374-375**, 239 (2006).
- ²⁰M. Fullgrabe, B. Ittermann, H. J. Stockmann, F. Kroll, D. Peters, and H. Ackermann, *Phys. Rev. B* **64**, 224302 (2001).
- ²¹C. P. Slichter, *Principles of Magnetic Resonance*, 2nd ed. (Springer-Verlag, Berlin, 1980).
- ²²P. de Trey, S. Gygax, and J.-P. Jan, *J. Low Temp. Phys.* **11**, 421 (1973).
- ²³W. Eckstein, *Computer Simulation of Ion-Solid Interactions* (Springer, Berlin, 1991).
- ²⁴J. D. Fletcher, A. Carrington, P. Diener, P. Rodiere, J. P. Brison, R. Prozorov, T. Olheiser, and R. W. Giannetta, *Phys. Rev. Lett.* **98**, 057003 (2007).
- ²⁵K. Ishida, Y. Niino, G. Zheng, Y. Kitaoka, K. Asayama, and T. Ohtani, *J. Phys. Soc. Jpn.* **65**, 2341 (1996).
- ²⁶W. A. MacFarlane, R. F. Kiefl, S. Dunsiger, J. E. Sonier, J. Chakhalian, J. E. Fischer, T. Yildirim, and K. H. Chow, *Phys. Rev. B* **58**, 1004 (1998).
- ²⁷R. F. Kiefl, W. A. MacFarlane, K. H. Chow, S. R. Dunsiger, T. L. Duty, T. M. S. Johnston, J. W. Schneider, J. E. Sonier, L. Brard, R. M. Strongin, J. E. Fischer, and A. B. Smith, *Phys. Rev. Lett.* **70**, 3987 (1993).